

# POTASSIUM ACCUMULATION AND PERMEATION IN THE CANINE CAROTID ARTERY

A. W. JONES *and* G. KARREMAN

*From the Bockus Research Institute and the Department of Physiology, University of Pennsylvania, Philadelphia, Pennsylvania 19146*

**ABSTRACT** Potassium accumulation was studied in slices equilibrated in solutions of varying potassium concentration ( $[K]_{ex} = 0-20$  mM). Steady-state  $^{42}K$  uptake was also measured under similar conditions. The accumulated potassium characterized by slow exchange kinetics (half time more than 25 min) exhibited saturation behavior at high external concentrations (maximum, 119 meq/kg dry solid), and exhibited *cooperative* interaction with sodium. Values calculated from an adsorption isotherm based on solute-protein interaction in a fixed charge system were in agreement with the experimental results. Rubidium competitively inhibited the accumulation of potassium. Studies of the  $^{42}K$  flux indicated that the rate constants for the slow component decreased with increasing  $[K]_{ex}$ . At  $[K]_{ex} = 3.33$  mM a minimum of about  $0.88 \times 10^{-4} \text{ sec}^{-1}$  was reached. The potassium flux exhibited saturation behavior at high  $[K]_{ex}$  (maximum  $10.5 \times 10^{-3} \text{ meq/kg d.s. per sec}$ ). A diffusion coefficient of  $1.1 \times 10^{-5} \text{ cm}^2 \text{ sec}^{-1}$  adequately characterized the fast exchanging potassium. A portion of this component exhibited saturation behavior (maximum, 11 meq/kg d.s.) and followed the Langmuir adsorption isotherm. The properties exhibited by potassium accumulation and permeation processes were consistent with those of a fixed charge system as formulated in the "association-induction hypothesis." It is suggested that this model provides an analytical basis for future experimentation.

## INTRODUCTION

Vascular smooth muscle is characterized by complex electrolyte exchange properties. In the preceding study both a fast component limited by bulk diffusion kinetics and a slower one following a reversible reaction were observed (Jones and Karreman, 1969). Under physiological conditions potassium was the predominant ion in the slow fraction. Relatively little information is available, however, relating potassium exchange and accumulation properties of smooth muscle to analytical models.

Numerous investigations of potassium exchange have been conducted on frog skeletal muscles. Most studies were based on the assumption of a resistive membrane separating two well mixed solutions of potassium. As noted by Harris and Sjodin (1961), this leads to the application of an exponential relation to describe the ex-

change processes. The steady-state exchange of potassium was demonstrated to be more complex, and a model was put forth by these investigators consisting of surface adsorption followed by inward diffusion (Harris and Sjodin, 1961; Sjodin, 1961). The exchange of electrolytes and nonelectrolytes in a variety of preparations follows Michaelis-Menton kinetics, indicating adsorption of exchanging molecules at sites on the surface or in the membrane (Rothstein, 1959; Wilbrandt and Rosenberg, 1961). The inclusion of aqueous channels in the model led to a "pump and leak" formulation (Wilbrandt and Rosenberg, 1961).

The predictions of several exchange models have been compared with measurements of the interactions of one alkali ion on the rate of entry of another in frog skeletal muscle (Ling and Ochsenfeld, 1965). Consideration of permeation data alone supported the models incorporating fixed charges with interspersed channels of polarized water either making up the membrane alone or distributed throughout the cell. Consideration of the accumulation properties led to the conclusions that insufficient sites are located in the membrane to accommodate the quantity of ions selectively accumulated, and that a model based on a cytoplasmic system of fixed charges and polarized water was more consistent (Ling and Ochsenfeld, 1965, 1966). Because the approach set forth by Ling (1962) and amplified in more recent work (Ling and Ochsenfeld, 1965, 1966; Ling, 1965, 1966 *a*, 1966 *b*) provided a basis for interrelating ion accumulation and permeation properties, this avenue was followed in the present work.

The objectives of the investigations were to systematically study potassium accumulation and permeation characteristics of the vascular wall and to test the applicability of a fixed charge model based on the "association-induction hypothesis" (Ling, 1962). In testing the model it was desired to compare experimental findings with values computed from analytical relations based on the physical model. Although the approach considered the associational properties of ions and proteins distributed throughout the cell, it would be of general applicability to subcellular systems which still maintain associational properties. The preparation employed had certain advantages for the studies undertaken. Almost all the initial potassium could be extracted by overnight cold storage, and subsequent incubation at 37°C for 3 hr resulted in stable potassium levels allowing the measurement of steady-state exchange (Jones and Karreman, 1969). This permitted the convenient study of low external potassium and of competing ions without employing prolonged tissue culture techniques. The properties exhibited by the potassium accumulation and permeation processes (saturation behavior, competitive inhibition, and *cooperative* interaction) were consistent with the "association-induction hypothesis."

A crucial aspect of the model is the reinforcement of selectivity in the protein sites resulting from inductive propagation of changes in polarizability of intervening atoms. Such reinforcement is essential for true *cooperative* phenomena, and distinguishes this mechanism from that considered for allosteric transitions by Monod

et al. (1965). They inferred "cooperativity" from the curvature of the "saturation function" for low concentrations of the ligand. The application of these two mechanisms to oxygen-hemoglobin dissociation curves indicates that the data can be fitted at least as well by either approach (Ling, 1966 *a*; Monod et al., 1965). It may be pointed out, however, that the adsorption isotherm based on the "association-induction hypothesis" required two parameters to be optimized, whereas the saturation function based on allosteric transitions required three.

## METHODS

The dogs and the handling of the carotid slices used in these experiments were the same as in the experiments discussed in the previous paper (Jones and Karreman, 1969). Solutions were also prepared in a similar manner with the resulting concentrations:  $\text{Na}^+$ , 145 mM;  $\text{K}^+$ , 4.5 mM;  $\text{Mg}^{2+}$ , 1.2 mM;  $\text{Ca}^{2+}$ , 2.5 mM;  $\text{Cl}^-$ , 126.3 mM;  $\text{HCO}_3^-$ , 22.5 mM;  $\text{SO}_4^{2-}$ , 3.45 mM;  $\text{H}_2\text{PO}_4^-$ , 1.2 mM and a glucose concentration of 5.5 mM with a gas phase of 95%  $\text{O}_2$  and 5%  $\text{CO}_2$  at 37°C. Variations in external potassium were achieved by adding or subtracting the appropriate amounts of KCl. A combination of metabolic inhibitors was employed similar to that in the preceding work.

The tissues were analyzed using standard techniques. In those experiments in which rubidium was present, sodium, potassium, and rubidium were analyzed on an atomic absorption spectrometer (Perkin-Elmer Corp., Norwalk, Conn., Model 303). Standards were employed with ion concentration ratios similar to those of the unknowns and containing 225 ppm Li as a radiation buffer.

For the study of  $^{42}\text{K}$  entry, slices were incubated in nonradioactive solutions at 37°C for 3 hr to achieve a steady state. The slices were then transferred to identical medium containing the isotope for periods of 1 min to 3 hr. Appropriate amounts of KCl were omitted from the loading medium to allow for the KCl added as carrier with the isotope. The slices and solutions were analyzed as in the preceding study (Jones and Karreman, 1969). The fraction exchanged was calculated by dividing the specific activity of the tissue potassium by that of the loading solution, and has been designated  $^{42}\text{K}/\text{K}_T$ .

## RESULTS

### *Potassium Accumulation*

The relation between potassium accumulation and external potassium concentration was studied under metabolically supported and inhibited conditions. The total potassium contents of the arterial wall were measured at nine levels of external potassium and are plotted in Fig. 1. Under metabolically inhibited conditions the potassium content was linearly related to the external concentration (slope = 4 liters/kg dry solid). Under metabolically supported conditions, however, the relation was more complex. At any given external potassium concentration the amount accumulated by the tissue exceeded that under the inhibited conditions ( $P < 0.001$ ). This was observed in the previous study at a physiological potassium concentration (Jones and Karreman, 1969). It was noted as well that the potassium exchange under metabolically supported conditions can be described in terms of two processes: bulk diffusion and a reversible reaction which could be described as an adsorption-desorption process (Jones and Karreman, 1969). The former process was characterized

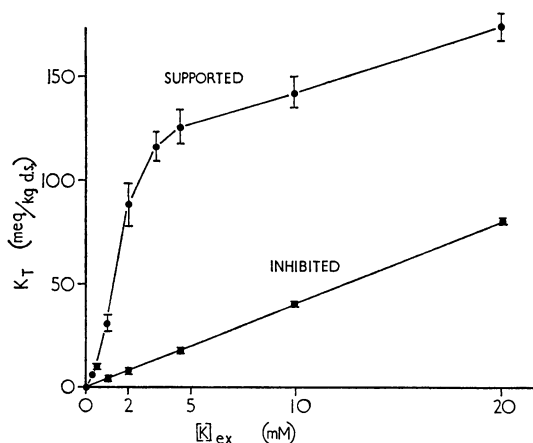


FIGURE 1 Total potassium contents under metabolically supported and inhibited conditions in equilibrium with various external potassium concentrations ( $[K]_{ex}$ ) at 37°C. Average values for supported conditions (13 dogs) and for inhibited conditions (7 dogs) joined by straight lines. Vertical bars represent  $\pm 1$  standard error of mean.

TABLE I  
EXPERIMENTAL DATA FOR  $^{42}K$  FLUX

$[K]_{ex}$	No. of dogs	$f_{slow}^*$	$1-f_{3min}^\dagger$	$\frac{1-f_{3min}}{f_{3min}}$	$\mu \times 10^{-4} \text{ sec}^{-1}$	K exchanged in 3 min
<i>mM</i>						<i>meq/kg d.s.</i>
0.33	4	0.70	0.74 $\pm 0.02$	2.9	3.85	1.2 $\pm 0.1$
0.5	4	0.78	0.81 $\pm 0.04$	4.3	2.89	1.8 $\pm 0.2$
1.0	6	0.82	0.84 $\pm 0.03$	5.2	2.18	3.8 $\pm 0.2$
2.0	4	0.90	0.91 $\pm 0.01$	10.1	1.54	7.6 $\pm 1.6$
3.33	4	0.88	0.87 $\pm 0.03$	6.7	0.84	12.4 $\pm 0.6$
4.5	4	0.88	0.87 $\pm 0.02$	6.7	0.88	15.5 $\pm 1.8$
10.0	4	0.75	0.74 $\pm 0.02$	2.8	0.89	31.0 $\pm 1.4$
20.0	4	0.58	0.63 $\pm 0.04$	1.7	0.90	55.1 $\pm 3.8$

$\pm$  Standard error of mean.

\* The value of  $1-(^{42}K/K_T)$  determined by extrapolating the lines in Figs. 7 and 8 to zero time.

† The value of  $1-(^{42}K/K_T)$  at 3 min incubation.

by a relatively fast exchange; the latter was much slower. Furthermore, under metabolically inhibited conditions only diffusion limited exchange was present. The proportionality between extracellular potassium concentration and tissue levels under inhibited conditions was consistent with this observation.

In order to evaluate the relation between external potassium and the quantity of potassium which exchanged via an adsorption-desorption process, it was necessary

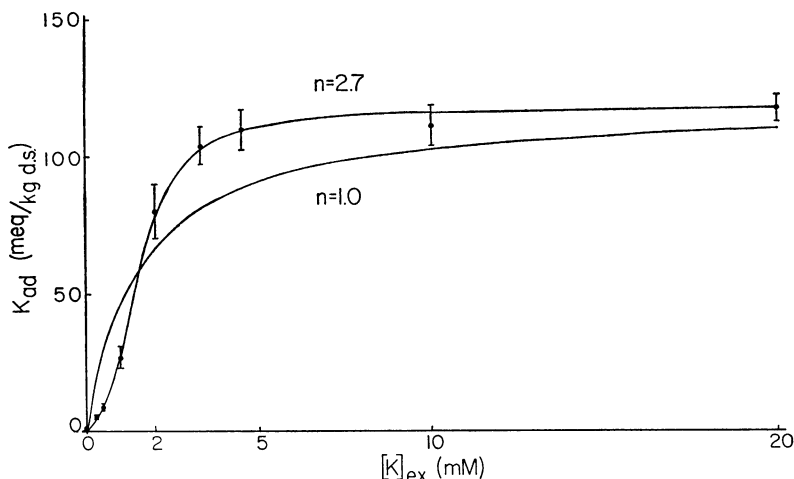


FIGURE 2 Adsorbed potassium contents in equilibrium with various  $[K]_{ex}$  at  $37^{\circ}\text{C}$ . Vertical bars represent  $\pm 1$  standard error of mean. Theoretical curves computed from equation (1) for  $n = 2.7$  and  $n = 1.0$ .

to correct the total electrolyte for the diffusion limited component. The entry of  $^{42}\text{K}$  under similar conditions exhibited a shoulder between 3 and 5 min (Fig. 10), indicating the diffusion limited component to be in equilibrium. The total potassium contents were corrected for the quantity exchanged in 3 min (Table I) and are plotted in Fig. 2. The accumulated potassium exhibited saturation behavior at high external concentrations in that an upper limit was approached. This behavior was consistent with that of a fixed charge system.

The accumulation of potassium by frog skeletal muscle has been described in terms of a solute-protein interaction, and the adsorption isotherm derived for such a system was applied to these data (Ling, 1965, 1966 *a*; Karreman, 1965). This isotherm took into account not only saturation properties but also *cooperative* interaction between protein and associated solute. For example, the exchange of a potassium ion for sodium at one adsorption site was regarded as influencing the free energy of adsorption at the nearest neighboring site. For each new  $\text{K}^+\text{-Na}^+$  pair formed, there would be an additional change of free energy referred to as the *free energy of nearest neighbor interaction* and designated  $-\gamma/2$  (Karreman, 1965; Ling, 1965, 1966 *a*). The *cooperative* adsorption isotherm for potassium in the presence of sodium is:

$$K_{ad} = \frac{F^- \tau}{2} \left\{ 1 + \frac{\frac{[K]_{ex}}{[Na]_{ex}} K_{K,Na} - 1}{\left[ \left( \frac{[K]_{ex}}{[Na]_{ex}} K_{K,Na} - 1 \right)^2 + 4 \frac{[K]_{ex}}{[Na]_{ex}} K_{K,Na} n^{-2} \right]^{1/2}} \right\} \quad (1)$$

where  $K_{ad}$  = adsorbed potassium, meq/kg d.s.;  $F^- \tau$  = total fixed charge available, meq/kg d.s.;  $K_{K,Na}$  = intrinsic equilibrium constant;  $n$  = an interaction parameter;

$[\text{Na}]_{\text{ex}}$  = external sodium concentration, meq/liter;  $[\text{K}]_{\text{ex}}$  = external potassium concentration, meq/liter. It has been noted (Karreman, 1965; Ling, 1965, 1966 a) that

$$n = \exp \left( - \frac{\gamma}{2RT} \right) \quad (2)$$

where  $-\gamma/2$  = free energy change of nearest neighbor interaction, kcal/mole;  $R$  = gas constant, kcal/mole per  $^{\circ}\text{C}$ ;  $T$  = absolute temperature,  $^{\circ}\text{K}$ . According to this approach, when  $n > 1$ ,  $-\gamma/2 > 0$ , the free energy change favors the adsorption of the same solute at two adjacent sites, and the process is referred to as "autocooperative" adsorption. When  $n < 1$ ,  $-\gamma/2 < 0$ , the process is referred to as "heterocooperative" adsorption. When  $n = 1$ ,  $-\gamma/2 = 0$ , equation (1) reduces to the familiar Langmuir adsorption isotherm:

$$K_{\text{ad}} = \frac{F_{-T} [\text{K}]_{\text{ex}} K_{\text{K,Na}}}{[\text{K}]_{\text{ex}} K_{\text{K,Na}} + [\text{Na}]_{\text{ex}}} \quad (3)$$

The parameters for equation (1) were derived from the experimental data in Fig. 2. The total sites available,  $F_{-T}$ , were estimated from the asymptote approached at high external concentrations and equaled 119 meq/kg d.s. The value for  $K_{\text{K,Na}}$  was calculated from the external potassium concentration (1.56 mM) required for half saturation of the accumulation ( $K_{\text{ad}} = F_{-T}/2$ ). At that concentration,

$$\frac{[\text{K}]_{\text{ex}}}{[\text{Na}]_{\text{ex}}} K_{\text{K,Na}} - 1 = 0 \quad (4)$$

and  $K_{\text{K,Na}} = 93$ . This represents an intrinsic free energy for  $\text{K}^+$ - $\text{Na}^+$  ion adsorption ( $\Delta F^{\circ}_{\text{K,Na}}$ ) of  $-2.8$  kcal/mole  $[K_{\text{K,Na}} = \exp \{ - (\Delta F^{\circ}_{\text{K,Na}}/RT) \}]$ .

The interaction parameter,  $n$ , was determined from a plot of  $\log X_{\text{K}}/(1 - X_{\text{K}})$  versus  $\log [\text{K}]_{\text{ex}}/[\text{Na}]_{\text{ex}}$ , where  $X_{\text{K}}$  is the mole fraction of sites occupied by potassium ( $K_{\text{ad}}/F_{-T}$ ). Over the middle range of values  $[X_{\text{K}}/(1 - X_{\text{K}}) = 1]$  it has been shown that the slope equals  $n$ , which in this study was 2.7 (Karreman, 1965; Ling, 1965, 1966 a; Karreman and Jones, 1965). This value represents an energy of nearest neighbor interaction of  $-\gamma/2 = 0.61$  kcal/mole. Since  $n$  was greater than 1, corresponding to a positive value for  $-\gamma/2$ , the interaction between  $\text{K}^+$  and  $\text{Na}^+$  ions was an *autocooperative* process. That is, as the potassium content increased under higher external concentrations, the accumulation of succeeding potassium ions became more favorable.

The calculated values for  $K_{\text{ad}}$  using equation (1) with the derived parameter values are presented in Table II and plotted in Fig. 2, and represent good agreement between theory and experiment. It may be noted that the experimental values for  $K_{\text{ad}}$  at low  $[\text{K}]_{\text{ex}}$  (0.33 and 0.5 mM) were not used in deriving values for  $F_{-T}$ ,  $K_{\text{K,Na}}$ , and  $n$ . These values for  $K_{\text{ad}}$  were, however, accurately predicted by equation (1). As a comparison, the Langmuir adsorption isotherm (no *cooperative* interaction) was

TABLE II  
EXPERIMENTAL AND CALCULATED ADSORBED CATION CONTENTS

$[K]_{ex}$	$Na_{ad}$	$K_{ad}$	Calculated $K_{ad}$
mm	meq/kg d.s.		
0	$152 \pm 12$	$0.8 \pm 0.2$	0
0.33	$129 \pm 8$	$5.0 \pm 0.8$	4.9
0.5	$126 \pm 9$	$8.7 \pm 1.3$	8.8
1.0	$120 \pm 11$	$27.0 \pm 3.8$	28.6
2.0	$23 \pm 12$	$80.7 \pm 9.5$	78.3
3.33	$27 \pm 12$	$103.9 \pm 6.8$	103.2
4.5	$24 \pm 9$	$109.9 \pm 7.7$	109.0
10.0	$33 \pm 11$	$111.3 \pm 7.3$	115.8
20.0	$6 \pm 13$	$117.6 \pm 5.1$	117.7

$\pm$  Standard error of mean for 13 experiments.

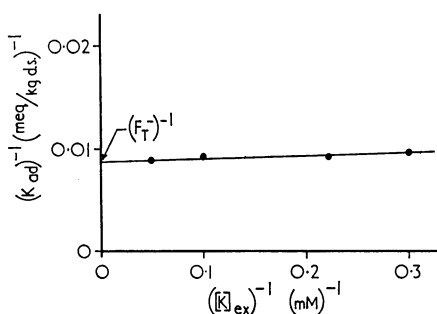


FIGURE 3 Reciprocal plot of adsorbed potassium and  $[K]_{ex}$ . Intercept represents total available sites ( $F_T$ ). Theoretical line computed from equation (3).

also plotted in Fig. 2. Significant differences between theory and experimental results were noted and were especially apparent at low external potassium concentrations, where even the curvature of the Langmuir adsorption isotherm was different from that of the experimental data.

In order to estimate the equilibrium constant with potassium occupying most of the nearest neighboring sites ( $K_{K,Na}$ ), the data in Fig. 2 were replotted in Fig. 3 for  $[K]_{ex} \geq 3.33$  mM. The straight line represents the calculated values for equation (3) using  $F_T = 119$  meq/kg d.s. and a derived value of  $K_{K,Na} = 305$ . This represented a free energy for potassium adsorption of  $-3.5$  kcal/mole.

The adsorbed sodium under conditions of varying external potassium concentration would be expected to equal the difference between the total available sites and those occupied by potassium. This analysis assumed the concentration of unoccupied sites to be negligible. The adsorption isotherm for sodium would therefore follow the equation:

$$Na_{ad} = \frac{F_T}{2} \left\{ 1 - \frac{\frac{[K]_{ex}}{[Na]_{ex}} K_{K,Na} - 1}{\left[ \left( \frac{[K]_{ex}}{[Na]_{ex}} K_{K,Na} - 1 \right)^2 + 4 \frac{[K]_{ex}}{[Na]_{ex}} K_{K,Na} n^{-2} \right]^{1/2}} \right\}. \quad (5)$$

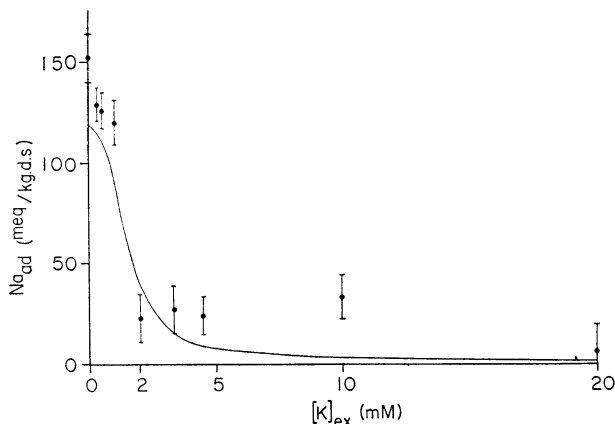


FIGURE 4 Adsorbed sodium contents in equilibrium with various  $[K]_{ex}$  and  $[Na]_{ex} = 145$  mM at  $37^{\circ}\text{C}$ . Vertical bars represent  $\pm 1$  standard error of mean. Theoretical curves computed from equation (5) for  $n = 2.7$ .

The adsorbed sodium contents were estimated by subtracting the rapidly exchanging component from the total sodium. In the preceding work the fast exchanging sodium was measured at  $[K]_{ex} = 0$  and  $[K]_{ex} = 4.5$  mM (Jones and Karreman, 1969). The adsorbed sodium was calculated by reducing the total by 307 meq/kg d.s. for  $[K]_{ex} \leq 1.0$  mM and by 388 meq/kg d.s. for  $[K]_{ex} > 1.0$  mM (Table IV in Jones and Karreman, 1969). The calculated experimental values and theoretical values from equation (5) appear in Fig. 4. Only two levels of adsorbed sodium were distinguishable which approximated the calculated values. It will be necessary to measure the fast exchanging sodium at intermediate  $(K)_{ex}$  to obtain a more precise comparison.

The potassium accumulation properties were further studied in the presence of an ion which was expected to act as a competitive inhibitor to potassium. Rubidium was chosen because it was found to have an association constant similar to that of potassium in skeletal muscle (Ling and Ochsenfeld, 1966). The adsorbed potassium values were calculated as before. The correction applied to the potassium data at  $[K]_{ex} = 4.5$  mM was applied to the rubidium content for all external potassium concentrations. The calculated experimental values are shown in Fig. 5. With increasing external potassium concentrations the adsorbed potassium levels increased while rubidium decreased. Under these conditions the sodium levels were relatively independent of the external potassium concentration. The Langmuir type of adsorption isotherm was applied to the data with values of  $F^{-\tau} = 126$  meq/kg d.s. and  $K_{K,Rb} = 0.68$ . The calculated values for  $K_{ad}$  and  $Rb_{ad}$  were plotted in Fig. 5 and good agreement was obtained.

It has recently been postulated that some fast exchanging potassium in the taenia coli may be accumulated via an adsorptive process (Goodford, 1966, 1967). The possibility of such adsorption in the arterial wall was evaluated by correcting the



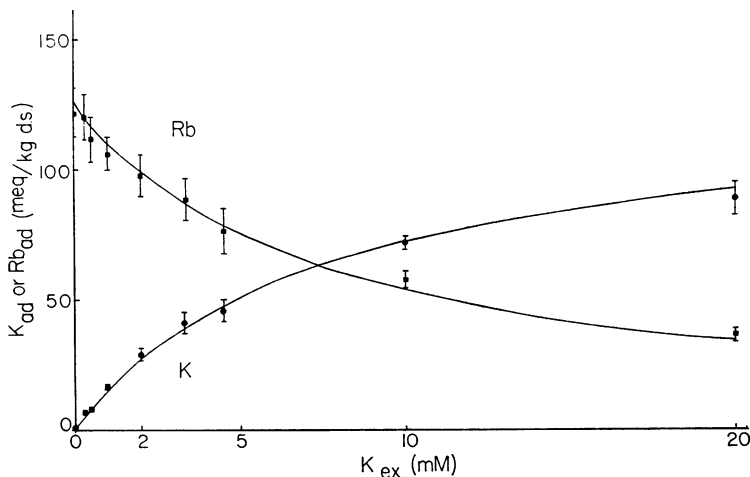


FIGURE 5 Adsorbed potassium and rubidium contents in equilibrium with various  $[K]_{ex}$  and  $[Rb]_{ex} = 5.0$  mM at  $37^{\circ}\text{C}$ . Average values (4 dogs) plotted with  $\pm 1$  standard error of mean. Theoretical curves computed from Langmuir adsorption isotherm, equation (3), with Na term replaced by Rb.

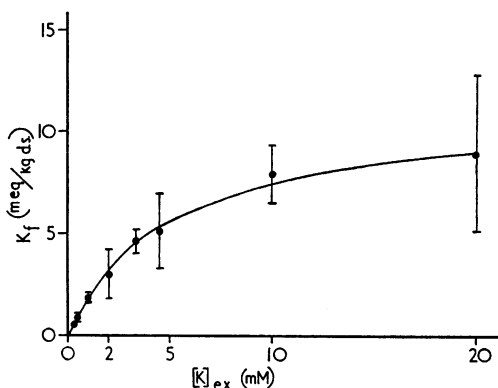


FIGURE 6 Fast exchanging potassium content not contained in sucrose space. Average values computed from data in table I. Vertical bars represent  $\pm 1$  standard error of mean. Theoretical curve computed from equation (3).

total fast exchanging potassium (Table I) for the quantity contained in the sucrose space (Jones and Karreman, 1969). This correction was considered to include the potassium dissolved in the extracellular water and some, but perhaps not all, of that dissolved in the interstitial cell water. The sucrose space of 1.86 kg  $\text{H}_2\text{O}$  per kg d.s. determined at  $[K]_{ex} = 0$  was used for  $[K]_{ex} \leq 1.0$  mM, and a space of 2.31 kg  $\text{H}_2\text{O}$  per kg d.s., determined at  $[K]_{ex} = 4.5$  mM, was applied to values for  $[K]_{ex} > 1.0$  mM (Jones and Karreman, 1969). The fast exchanging potassium calculated to be outside of the sucrose space was plotted in Fig. 6. The data exhibited saturation behavior and fell along a curve calculated with equation (3). The derived value for  $F^-_T$  was 11.0 meq/kg d.s. and for  $K_{K,Na}$ , 32. If all excess potassium were in solution, a linear relation would have been expected.

## Potassium Permeation

The steady-state entry of  $^{42}\text{K}$  was investigated under conditions similar to those employed in the accumulation studies. The data were plotted on a semilogarithmic graph to facilitate the analysis of the slow exchange process. Values for  $[\text{K}]_{\text{ex}} \leq 3.33$  mM appear in Fig. 7 and for  $[\text{K}]_{\text{ex}} \geq 4.5$  mM in Fig. 8. With increasing external concentration of potassium there was a decrease in the rate of exchange, reaching a minimum at  $[\text{K}]_{\text{ex}} = 3.33$  mM. At higher concentrations the rate of exchange was essentially constant. The fraction of the total potassium exchanging at a slow rate was also concentration dependent, reaching a maximum at  $[\text{K}]_{\text{ex}} = 2.0$  mM. Over the incubation periods tested, little deviation from a single exponential function was apparent. When applied over a period in which the slow fraction decreases to  $1/e$  of the initial value, this analysis yields the same value for the mean rate constant as an analysis based on a rate constant following a log normal distribution (Jones and

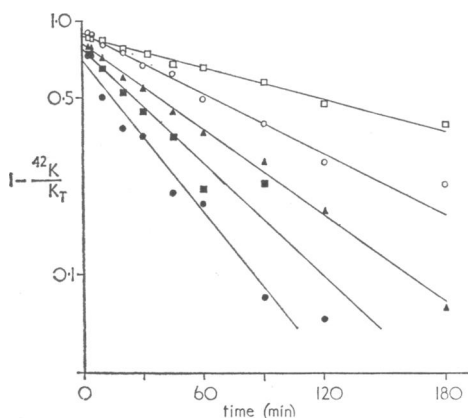


FIGURE 7 Steady-state exchange of tissue potassium ( $K_T$ ) with radioactive  $^{42}\text{K}$  solutions at  $37^\circ\text{C}$ . Abscissa, time of incubation in radioactive solution at  $[\text{K}]_{\text{ex}} = 0.33$  mM (solid circles), 0.5 mM (solid squares), 1.0 mM (triangles), 2.0 mM (open circles), and 3.33 mM (open squares). Logarithmic ordinate scale, average values (4 dogs for each concentration except 1.0 mM, 6 dogs) for 1 minus the fraction exchanged with isotope. Straight line represents single exponential fitted to slowly exchanging component.

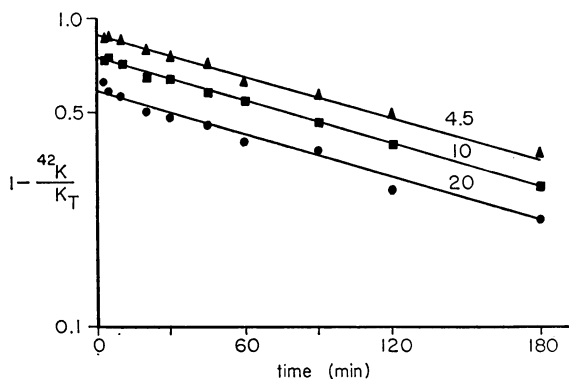


FIGURE 8 Steady-state exchange of tissue potassium with  $^{42}\text{K}$  solutions at  $37^\circ\text{C}$ . Plotted as in Fig. 7. Average values (4 dogs) for  $[\text{K}]_{\text{ex}} = 4.5$  mM (triangles), 10 mM (squares), and 20 mM (circles).

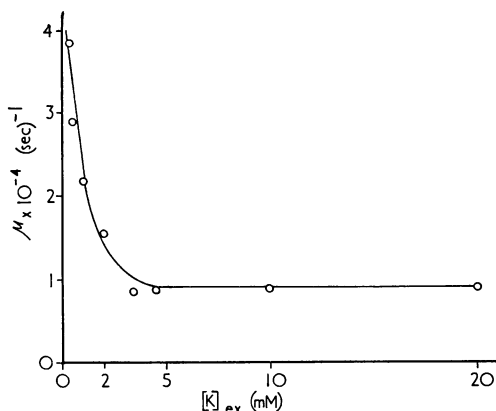


FIGURE 9 Rate constants for potassium exchange at various  $[K]_{ex}$ . Curve computed from equation (6).

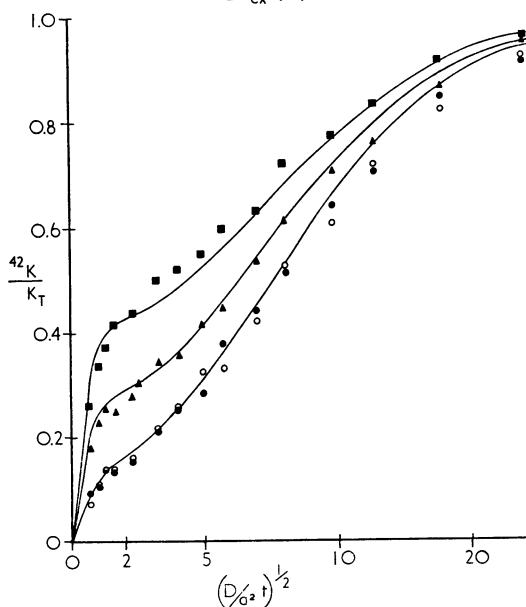


FIGURE 10 Steady-state exchange of tissue potassium with  $^{42}\text{K}$  solutions at  $37^\circ\text{C}$ . Abscissa, nondimensional time parameter. Ordinate, fraction exchanged. Values replotted from experiments shown in Fig. 7 and Fig. 8 for  $[K]_{ex} = 3.33$  mM (open circles), 4.5 mM (solid circles), 10 mM (triangles), and 20 mM (squares). Theoretical curves computed from bulk diffusion-reversible reaction equations for  $[K]_{ex} = 4.5$  mM, 10 mM, 20 mM.

Karreman, 1969; Creese et al., 1956). The derived constants for the  $^{42}\text{K}$  flux studies are presented in Table I. The dependence of the rate constant,  $\mu$ , on the external potassium concentration is more clearly demonstrated in Fig. 9. An empirical relation was fitted to the rate constants where

$$\mu = 0.88 \times 10^{-4} \text{ sec}^{-1} + 3.8 \times 10^{-4} \text{ sec}^{-1} e^{-[K]_{ex}}. \quad (6)$$

A kinetic model based upon bulk phase limited diffusion coupled with a reversible reaction was applied to  $^{42}\text{K}$  entry. This model has been described in relation to skeletal muscle and frog egg permeability (Ling, 1966 *b*; Ling, et al., 1967). It has been applied in the preceding paper to the analysis of ion entry into the arterial wall

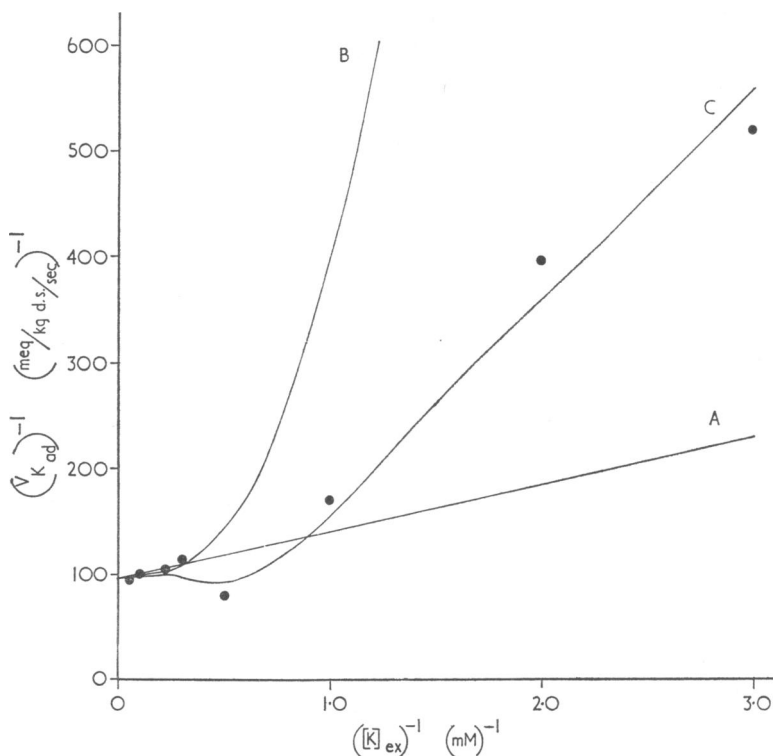


FIGURE 11 Reciprocal plot of potassium flux and  $[K]_{ex}$ . Theoretical curve *A* computed from equation (7), curve *B* from equation (8), and curve *C* from the reciprocal of the product of equations (1) and (6).

(Jones and Karreman, 1969). The analysis was based upon the theoretical treatment of Crank (1956). The experimental data and calculated curves for  $[K]_{ex} \geq 3.33 \text{ mM}$  are presented in Fig. 10. The values used for the diffusion coefficient,  $D$ , were  $1.1 \times 10^{-5} \text{ cm}^2 \text{ sec}^{-1}$ , and for  $a$ , the half thickness of the slice,  $0.035 \text{ cm}$ . A shoulder appeared in the curves and data at values of  $[(D/a^2)t]^{1/2}$  corresponding to the time required for the diffusion process to reach equilibrium. The reversible reaction was characterized in this model by a forward reaction,  $\lambda[K]_{ex}$ , and a backward reaction or desorption,  $\mu K_{ad}$ , where  $\lambda$  and  $\mu$  are rate constants. Under steady-state conditions the reactions are equal. The flux of the desorbed potassium,  $V_{Kad}$ , was calculated from the product of the rate constant for desorption at each  $[K]_{ex}$  (Table I) and the adsorbed potassium in equilibrium with that concentration (Table II). The dependence of the potassium flux upon external potassium is presented in Fig. 11. At high concentrations the flux approached a maximum. The plot of the data deviated markedly from a straight line at lower concentrations.

Three equations were fitted to the experimental results in Fig. 11. The one designated *A* was based upon Michaelis-Menton kinetics, in which

$$\frac{1}{V_{K_{ad}}} = \frac{1}{V_{max}} (K_m) \frac{1}{[K]_{ex}} + \frac{1}{V_{max}} \quad (7)$$

where  $V_{max}$  = maximum rate, meq/kg d.s. per sec;  $K_m$  = Michaelis constant, meq/liter. The values used for  $V_{max}$  were  $10.5 \times 10^{-3}$  meq/kg d.s. per sec, and for  $K_m$ , 0.47 meq/liter.

The second relation,  $B$ , was:

$$\frac{1}{V_{K_{ad}}} = \frac{1}{\mu K_{ad}} \quad (8)$$

where  $K_{ad}$  was calculated from equation (1) and  $\mu = 0.88 \times 10^{-4} \text{ sec}^{-1}$ , the rate constant approached at high external potassium concentration. In this relation  $V_{max} = \mu F_{-T}^-$ . The third relation,  $C$ , took into account the dependence of  $\mu$  upon  $[K]_{ex}$ , and  $V_{K_{ad}}$  was calculated from the product of equations (1) and (6). At high external potassium concentration,  $[K]_{ex} > 3.33 \text{ mM}$ , the three relations agreed with the experimental data. Beyond this range it was necessary to take into account the *cooperative* interaction between  $K^+$  and  $Na^+$  as well as the effects of  $[K]_{ex}$  upon the rate constants.

On the basis of the permeability data it is not possible to differentiate between potassium exchange limited by sites located on the surface and by those distributed throughout the cytoplasm. The parameters applied to curves  $B$  and  $C$  in Fig. 11 were based on a network of cytoplasmic sites. To reconstruct curve  $C$  with a surface limited model it would be necessary to decrease the value employed for  $F_{-T}^-$ , assuming the surface charge to be only a fraction of the total available, and to increase proportionally the value employed for the rate constant. The *cooperative* interaction between surface sites and the concentration dependence of  $\mu$  would be assumed to be similar to that derived for the cytoplasmic network. These latter properties, however, indicate that a membrane transport model employing Michaelis-Menton kinetics would not be of general applicability over the concentration range employed.

## DISCUSSION

The accumulation of potassium under metabolically supported conditions exhibited several properties of an interaction between ions and a proteinaceous fixed charge system. Saturation behavior was one such property. The levels attained were similar in the two studies in which the external potassium concentrations were varied. It would be expected that the saturation levels would be compatible with the available  $\beta$ -carboxyl groups of aspartic acid and  $\gamma$ -carboxyl groups of glutamic acid. This has been noted in other tissues and can be assumed to be a general property of smooth muscle as well (Ling, 1962; Ling and Ochsenfeld, 1966).

Another property of solute-protein interaction exhibited by vascular smooth muscle was that of *cooperative* interaction between  $K^+$  and  $Na^+$  ions. The interaction was of the *autocooperative* type. The value for the free energy of nearest neighbor interaction was similar to that found in skeletal muscle ( $-\gamma/2 = 0.6$  kcal/mole; Ling, 1966 a). Therefore, because of the *cooperative* interaction, the free energy of  $K^+$ - $Na^+$  ion adsorption for any site depended upon the ion associated to neighboring sites. The free energy for  $K^+$  adsorption with  $Na^+$  occupying a neighboring sites would be  $-2.8$  kcal/mole  $- (-0.61$  kcal/mole)  $= -2.2$  kcal/mole. This was equivalent to an equilibrium constant of  $\exp \{ - (-2.2/RT) \} = 35$ . The free energy and equilibrium constant with potassium occupying neighboring sites would be  $-2.8$  kcal/mole  $+ (-0.61$  kcal/mole)  $= -3.4$  kcal/mole with  $K_{K,Na} = 250$ . This value was in agreement with that derived from experimental values at high external potassium concentrations.

The ion accumulation mechanism exhibited competitive inhibition between the similarly associated ions,  $K^+$  and  $Rb^+$ . The intrinsic equilibrium constant indicated that vascular smooth muscle selectivity for the three cations studied was  $Rb^+ > K^+ \gg Na^+$ . This order was similar to that found in skeletal muscle (Ling and Ochsenfeld, 1966). In the case of the two similarly adsorbed ions ( $K_{K,Rb} \simeq 1$ ), *cooperative* interaction was essentially absent. Such a finding would indicate that the inductive effects of the two ions were also quite similar (Ling, 1962).

A second component which exhibited properties of a solute-fixed charge interaction was present in the arterial wall. It was characterized by fast exchange kinetics. The available sites were relatively few in comparison with the slowly exchanging component, but were of the same order as those calculated to be available on acid mucopolysaccharides (Jones and Karreman, 1969). On the basis of Goodford's work it also appears possible that the excess fast exchanging potassium is associated with the smooth muscle surface (Goodford, 1966, 1967). A more detailed investigation will be necessary to locate the constituents associated with this excess fast exchanging electrolyte and to evaluate its physiological role.

The steady-state potassium flux exhibited saturation behavior which was consistent with the view that potassium and sodium compete for a limited number of sites either located on the surface or distributed throughout the cytoplasm. An additional feature of this process was the dependence of the rate constants upon the external potassium concentration. It would appear that the *cooperative* interaction of  $K^+$  and  $Na^+$  ions on the fixed charge not only affects the free energy of adsorption, but also alters the activation energy required for desorption.

On the basis of the present and the preceding study, it appears that a model based on the associational properties of ions and proteins provides a reasonable approach to the derivation of quantitative relations for the ion exchange properties of the vascular wall (Jones and Karreman, 1969). As a result of this approach, the following equation can be written to represent potassium accumulated in the arterial wall:

$$K_T = [K]_{\text{ex}} V_{\text{ex}} + \left[ \frac{F^-_f [K]_{\text{ex}} K_{K,Na}}{[K]_{\text{ex}} K_{K,Na} + [Na]_{\text{ex}}} \right]_{\text{fast}} + q_K^{\infty \rightarrow \text{ins}} [K]_{\text{ex}} V_{\text{ins}} + \frac{F^-_T}{2} \left\{ 1 + \frac{\frac{[K]_{\text{ex}}}{[Na]_{\text{ex}}} K_{K,Na}^{-1}}{\left[ \left( \frac{[K]_{\text{ex}}}{[Na]_{\text{ex}}} K_{K,Na} - 1 \right)^2 + 4 \frac{[K]_{\text{ex}}}{[Na]_{\text{ex}}} K_{K,Na} n^{-2} \right]^{1/2}} \right\} \quad (9)$$

where  $K_T$  = total potassium, meq/kg d.s.;  $V_{\text{ex}}$  = volume of the extracellular fluid, about 2.1 liters  $\text{H}_2\text{O}$  per kg d.s. over the concentration range studied (Jones and Karreman, 1969);  $q_K^{\infty \rightarrow \text{ins}}$  = equilibrium distribution coefficient for dissolved potassium, on the basis of the sodium calculation estimated to be 0.24 (Jones and Karreman, 1969);  $V_{\text{ins}}$  = volume of the cell water, about 1.0 liter  $\text{H}_2\text{O}$  per kg d.s. over the concentration range studied (Jones and Karreman, 1969). The first three terms make up the bulk diffusion limited component, and the last term exhibits adsorption-desorption kinetics. It is realized that some of the parameters, such as  $q_K^{\infty \rightarrow \text{ins}}$ , can only be estimated at the present time. Also in a complex tissue such as the arterial wall more terms and factors, e.g. calcium, will have to be included as more detailed investigations are carried out. However, it is thought that this approach provides an analytical basis for treating the control of vessel wall water and electrolyte by hormonal and renal factors, as well as providing a basis for relating ion accumulation processes of the arterial wall to its mechanical properties.

The authors wish to thank Dr. L. H. Peterson for advice and discussion of this work; and Mr. M. L. Cole and Mr. R. P. Feeley for computer programing.

This work is supported by USPHS grant HE-07762 and ONR Grant 551 (54).

Received for publication 8 September 1968 and in revised form 18 March 1969.

## REFERENCES

- CRANK, J. 1956. *The Mathematics of Diffusion*. Clarendon Press, Oxford, England. 133.
- CREESE, R., M. W. NEIL, and G. STEPHENSON. 1956. *Trans. Faraday Soc.* **52**:1022.
- GOODFORD, P. J. 1966. *J. Physiol. (London)*. **186**:11.
- GOODFORD, P. J. 1967. *J. Physiol. (London)*. **192**:145.
- HARRIS, E. J., and R. A. SJODIN. 1961. *J. Physiol. (London)*. **155**:221.
- JONES, A. W., and G. KARREMAN. 1969. *Biophys. J.* **9**:884.
- KARREMAN, G. 1965. *Bull. Math. Biophys.* **27**:91.
- KARREMAN, G., and A. W. JONES. 1965. *Proceedings of the 18th Annual Conference on Engineering Medicine and Biology*. 26.
- LING, G. N. 1962. *A Physical Theory of the Living State*. Blaisdell Publishing Co., Waltham, Mass.
- LING, G. N. 1965. *Perspectives Biol. Med.* **9**:87.
- LING, G. N. 1966 a. *Federation Proc.* **25**:958.
- LING, G. N. 1966 b. *Ann. N. Y. Acad. Sci.* **137**:837.
- LING, G. N., and M. M. OCHSENFELD. 1965. *Biophys. J.* **5**:777.
- LING, G. N., and M. M. OCHSENFELD. 1966. *J. Gen. Physiol.* **49**:819.
- LING, G. N., M. M. OCHSENFELD, and G. KARREMAN. 1967. *J. Gen. Physiol.* **50**:1807.
- MONOD, J., J. WYMAN, and J. P. CHANGEUX. 1965. *J. Mol. Biol.* **12**:88.
- ROTHSTEIN, A. 1959. *Bacteriol. Rev.* **23**:175.
- SJODIN, R. A. 1961. *J. Gen. Physiol.* **44**:929.
- WILBRANDT, W., and T. ROSENBERG. 1961. *Pharmacol. Rev.* **13**:109.